Supporting Information for: Extraordinary Sunlight Absorption and 1 nm-Thick Photovoltaics using Two-Dimensional Monolayer Materials

Marco Bernardi,[†] Maurizia Palummo,[‡,†] and Jeffrey C. Grossman[*,†]

Department of Materials Science and Engineering, Massachusetts Institute of Technology, 77 Massachusetts Avenue, Cambridge MA 02139-4307, USA, and Dipartimento di Fisica, Università di Roma Tor Vergata, CNISM, and European Theoretical Spectroscopy Facility (ETSF), Via della Ricerca Scientifica 1, 00133 Roma, Italy

E-mail: jcg@mit.edu

[*]To whom correspondence should be addressed

[†]Department of Materials Science and Engineering, Massachusetts Institute of Technology, 77 Massachusetts Avenue, Cambridge MA 02139-4307, USA

[‡]Dipartimento di Fisica, Università di Roma Tor Vergata, CNISM, and European Theoretical Spectroscopy Facility (ETSF), Via della Ricerca Scientifica 1, 00133 Roma, Italy

Methods

We performed *ab initio* DFT, GW, and Bethe Salpeter calculations using the Vienna Ab Initio Simulation Package (VASP),[1,2] as detailed below.

TMD, graphene, and bilayer structures. Monolayer TMD were modeled using experimental lattice constants as in ref.,[3] and further relaxed within DFT. This approach is known to give accurate physical properties, such as direct DFT band gaps as well as accurate Raman shifts.[3,4] For monolayer graphene, a relaxed lattice constant of 2.48Å was used. The bilayer structures were relaxed using the van der Waals functional from Grimme[5] as implemented in the VASP code. For the MoS_2/graphene bilayer, a 4x4 hexagonal supercell of MoS_2 with experimental lattice constants was placed at a van der Waals distance of 3.3Å from a 5x5 hexagonal supercell of graphene, adopting the so-called TS stacking with C atoms on top of S atoms in MoS_2 (see ref.[6]). To achieve in-plane structural matching, a 1.3% strain was imposed in the graphene layer. We have verified that 1) this strain does not affect the bandstructure of graphene, and 2) the relaxed and unrelaxed bilayer structures yield the same bandstructures and Schottky barriers to within a few meV. The MoS_2/WS_2 bilayer unit cell consisted of stacked three-atom unit cells of the two monolayers. The experimental lattice parameters of MoS_2 were adopted, and the two layers were arranged with AB stacking (also called C7 stacking, see ref.[7]). Since the experimental lattice constants of MoS_2 and WS_2 are almost identical,[3] this choice led to a negligible strain in the WS_2 layer. In both the monolayer and bilayer cases, spurious interactions with the image systems were avoided by using $>$18Å vacuum in the layer-normal direction, consistent with previous work[3,8,9] and leading to converged results at all levels of theory used in this work.

DFT calculations. Commonly employed *ab initio* calculations in the framework of density functional theory (DFT) are limited to quantities related to the electronic ground state, whereas excited state phenomena − such as photoabsorption − need more accurate treatment of electron-electron and electron-hole correlation.[10,11] DFT is employed in this work within the GGA approx-

imation as a starting point to compute the Kohn-Sham wavefunctions and eigenvalues in unit cells of monolayer MoS_2, $MoSe_2$, and WS_2, using a plane wave basis set and periodic boundary conditions. Similar calculations have been previously shown to yield qualitatively correct bandstructures for monolayer TMD, featuring a direct gap at the K point responsible for the optical absorption onset.[8,12,13] We employ the GW method[14] and the Bethe-Salpeter equation (BSE)[11] as two subsequent levels of theory to obtain the macroscopic dielectric tensor including an accurate account of electron-electron and electron-hole interactions. We apply the GW method perturbatively, using so-called G_0W_0 calculations to obtain first-order corrections to the DFT eigenvalues, suitable as a starting point for BSE. We employed the PBE exchange-correlation functional[15] in combination with projector augmented wave (PAW) type pseudopotentials as implemented in the VASP package.[16,17] The GW version of the PAW pseudopotentials supplied by VASP was employed for all atoms, providing accurate scattering properties at high energies.[2] In the study of the TMD materials, the PAW pseudopotentials represented the nuclei plus core electrons up to the $3d$ shell for Mo (thus explicitly including the $4s$ and $4p$ semicore electrons in the calculation) and up to the $5s$ shell for W (thus including the $5p$ semicore electrons in the calculation), while for S and Se atoms only the s and p electrons of the outermost shell were included. While the explicit inclusion of semicore electrons for the transition metals Mo and W does not affect the DFT bandstructure, it is crucial to obtain a correct treatment of the exchange part of the self-energy at the G_0W_0 level of theory. We have verified for the case of MoS_2 that neglecting to include such semicore electrons in the calculation leads to erroneous G_0W_0 corrections with strong $\vec{k}$-dependence, and to indirect quasiparticle gaps due to inadequate treatment of the exchange energy; while all the calculations shown here were performed using the VASP code, these test calculations without semicore electrons were carried out using the Yambo code[18] coupled to DFT calculations using Quantum Espresso.[19]We employed kinetic energy cutoffs of up to 450 eV, and obtained spin-orbit split bandstructures by using the LSORBIT tag in VASP with quantization axis in the plane-normal direction. We first performed a self-consistent calculation using a $32\,\mathrm{x}\,32\,\mathrm{x}\,1$ Γ-centered Monkhorst-Pack[20] $\vec{k}$-point grid and with a strict tolerance of 10^{-8}eV on the total energy to obtain an accurate ground state charge

density. Subsequently, we performed non-selfconsistent calculations with Γ-centered $\vec{k}$-point grids of up to 24 x 24 x 1 and over 170 empty bands to obtain Kohn-Sham wavefunctions and eigenvalues as a starting point for optical absorption calculations using the GW-Bethe Salpeter method (see below).

For the calculation of workfunctions and Schottky barriers, we averaged the Hartree potential in the layer-normal direction and computed the Fermi energy for the monolayer or bilayer under study. The workfunction was obtained as the difference between the vacuum Hartree potential and the Fermi energy. The Schottky barrier at the MoS_2/graphene interface was computed as the difference between the Fermi energy of the bilayer and the VBM energy in an isolated MoS_2 monolayer, corrected by the interface dipole potential as detailed in the work by Shan *et al.*[21] This approach is analogous to obtaining the Schottky barrier from the PDOS, by taking the difference of the Fermi energy and the VBM in the bilayer calculation. For the MoS_2/WS_2 interface, the type-II alignment was determined from the nature of the VBM and CBM in the PDOS, and would also be found at the GW and BSE levels of theory as explained in the main text.

GW-Bethe Salpeter calculations. GW quasiparticle calculations were carried out using the perturbative ("one-shot") G_0W_0 approximation, starting from PBE Kohn-Sham wavefunctions and eigenvalues as described above. The energy cutoff for the response function was set to 150 eV, and increasing it up to 400 eV did not change the results for a fixed number (184) of empty bands. Our convergence study for TMD monolayers within the VASP implementation of GW is consistent with previous work,[8] and our computed GW bandstructures and energy gaps agree with the literature.[8,9] Calculations of the macroscopic dielectric tensor within the BSE framework were performed starting from G_0W_0 eigenvalues and PBE Kohn-Sham wavefunctions (since the perturbative G_0W_0 scheme used here does not update the wavefunctions). A 16 x 16 x 1 Γ-centered Monkhorst-Pack[20] $\vec{k}$-point grid was used in the calculation of the BSE spectra in Figure 1, and spin-orbit effects were included as explained above. We have verified carefully the convergence of the absorption spectrum with respect to the density of the $\vec{k}$-grid. We observed only slight variations between a 12 x 12 x 1 grid and the 16 x 16 x 1 grid employed for the spectra in Figure 1. Separate convergence

tests of the BSE spectra were performed without spin-orbit employing $\vec{k}$-grids of up to 24 x 24 x 1, confirming that an adequate convergence can be achieved for $\vec{k}$-grids of 12 x 12 x 1 and denser. The BSE Hamiltonian was formed using the six highest valence bands and the eight lowest conduction bands using the Tamm-Dancoff approximation, and the dielectric tensor was output on a fine energy grid (2,000 points) up to 8 eV. Our methodology is similar to ref.,[8] but employs significantly denser k-grids in the Brillouin zone leading to full convergence of the dielectric matrix. For the three TMD monolayers, we observe optical gaps slightly exceeding the experimental value, likely due to finite temperature effects in the experiment, or to self-interaction errors in the Kohn-Sham orbitals.[8] To predict the correct absorption at room temperature, we limited ourselves to slightly red-shifting the optical spectrum by $\sim$100$-$200 meV to match the experimental absorption onset of each monolayer TMD studied here. This approach is sufficiently accurate for the scope of this work, as confirmed by the agreement with the experimental data (see Figure 1b).

Absorbance calculations. The procedure outlined above yields the imaginary part of the dielectric tensor $\varepsilon_2(\omega)$ as a function of photon frequency ω, at energies relevant for interband optical transitions. Starting from $\varepsilon_2(\omega)$, the monolayer absorbance $A(\omega)$ of monolayer TMD, defined as the fraction of photons of energy $E = \hbar\omega$ absorbed by the monolayer, is obtained using an approximation analogous to what used by Yang *et al.* for graphene:[22]

$$A(\omega) = \frac{\omega}{c}\varepsilon_2 \Delta z \tag{1}$$

where c is the speed of light, and Δz is the size of the simulation cell in the layer-normal direction. This formula can be seen as a Taylor expansion for small thickness $\Delta z \to 0$ of the absorbance $A = 1 - e^{-\alpha \cdot \Delta z}$ for a flat layer of a bulk material with thickness Δz and absorption coefficient[23] $\alpha(\omega) = \frac{\varepsilon_2 \omega}{cn}$, with refractive index $n = 1$ due to the presence of vacuum in the vast majority of the simulation cell. Equivalently, it can be seen as deriving from the polarizability per unit area,[22] or from the optical conductivity of the monolayer. The absorbance defined with this approach is independent of the simulation cell size, since $\varepsilon_2 \propto (\Delta z)^{-1}$ when a large vacuum is introduced.

The ε_2 and absorbance for the MoS_2/graphene interface were computed within DFT using the independent-particle (DFT-RPA) approximation (rather than BSE), since the large size of the system (616 valence electrons) makes it impossible to apply BSE calculations in this case. Since DFT-RPA spectra usually underestimate the absorbance at low energies near the onset (as observed here, see Figure S1), our approach ensures a *conservative* estimate of J_{sc} and PCE for the MoS_2/graphene interface. This is confirmed by the fact that the sum of the BSE absorbances leads to a 30% higher J_{sc} current than the DFT-RPA result, as discussed in the main text.

Supplementary Figures

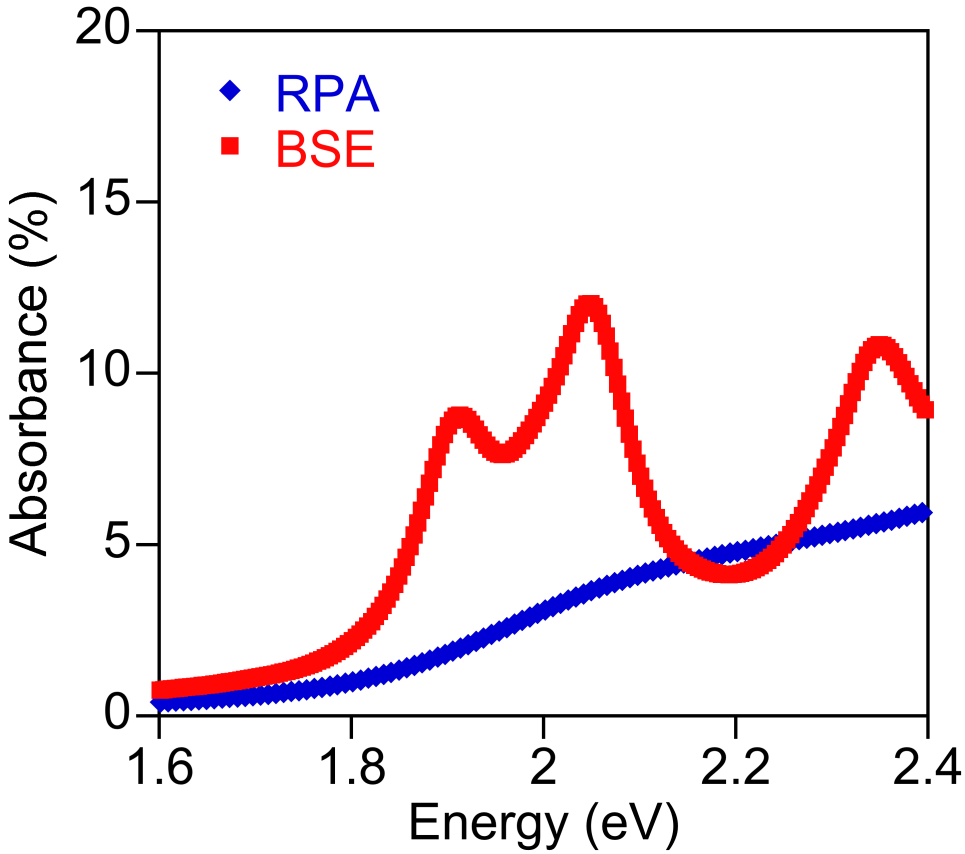

Figure S1. Absorbance of monolayer MoS_2 computed using different approximations. Shown are the DFT independent particle random-phase approximation (DFT-RPA) and the Bethe-Salpeter equation (BSE) absorbance spectra. The BSE theory includes excitonic effects, which lead here to a significant increase in the absorbance at visible photon energies. For the sake of comparing the two absorbance spectra, the DFT-RPA spectrum was shifted by +200 meV and the BSE by -200 meV (see above) to match the experimental gap of monolayer MoS_2.

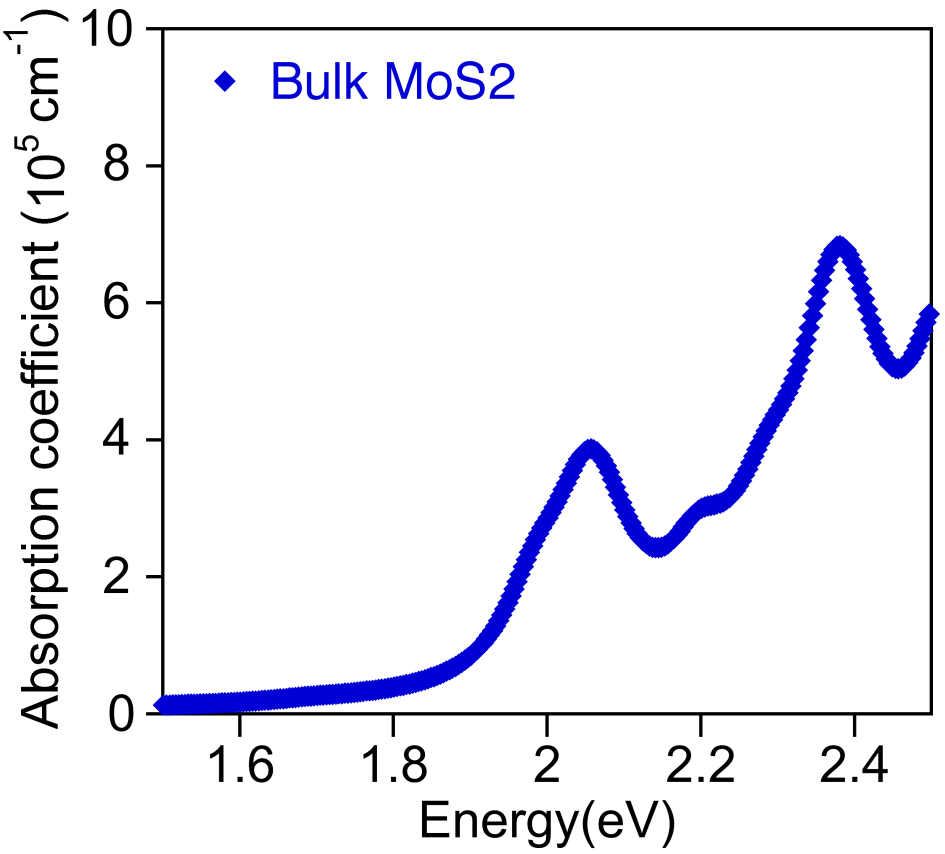

Figure S2. Absorption coefficient α for bulk MoS_2. The formula $\alpha(\omega) = \frac{\omega \cdot \varepsilon_2(\omega)}{c \cdot n(\omega)}$ was employed, where $\varepsilon_2(\omega)$ and $n(\omega)$ were both computed using BSE. The spectrum was shifted by -200 meV similar to the MoS_2 monolayer case. Values of $\alpha = 1-6 \cdot 10^5$ cm^{-1} are found at visible energies of up to 2.5 eV, in excellent agreement with the measured absorption spectrum for bulk MoS_2 (see ref.[24]).

References

(1) Kresse, G.; Furthmüller, J. *Phys. Rev. B* **1996**, *54*, 11169.

(2) Shishkin, M.; Kresse, G. *Phys. Rev. B* **2006**, *74*, 035101.

(3) Ramasubramaniam, A.; Naveh, D.; Towe, E. *Phys. Rev. B* **2011**, *84*, 205325.

(4) Ataca, C.; Topsakal, M.; AktuÌĺrk, E.; Ciraci, S. *J. Phys. Chem. C* **2011**, *115*, 16354–16361.

(5) Grimme, S. *J. Comp. Chem.* **2006**, *27*, 1787–1799.

(6) Ma, Y.; Dai, Y.; Guo, M.; Niu, C.; Huang, B. *Nanoscale* **2011**, *3*, 3883–3887.

(7) Kośmider, K.; Fernández-Rossier, J. *ArXiv e-prints* **2012**,

(8) Ramasubramaniam, A. *Phys. Rev. B* **2012**, *86*, 115409.

(9) Cheiwchanchamnangij, T.; Lambrecht, W. R. L. *Phys. Rev. B* **2012**, *85*, 205302.

(10) Martin, R. M. *Electronic Structrure: Basic Theory and Practical Methods*; Cambridge University Press, 2008.

(11) Onida, G.; Reining, L.; Rubio, A. *Rev. Mod. Phys.* **2002**, *74*, 601–659.

(12) Li, T.; Galli, G. *J. Phys. Chem. C* **2007**, *111*, 16192–16196.

(13) Splendiani, A.; Sun, L.; Zhang, Y.; Li, T.; Kim, J.; Chim, C.-Y.; Galli, G.; Wang, F. *Nano Lett.* **2010**, *10*, 1271–1275.

(14) Hybertsen, M. S.; Louie, S. G. *Phys. Rev. B* **1986**, *34*, 5390–5413.

(15) Perdew, J.; Burke, K.; Ernzerhof, M. *Phys. Rev. Lett.* **1996**, *77*, 3865.

(16) Blöchl, P. E. *Phys. Rev. B* **1994**, *50*, 17953.

(17) Kresse, G.; Joubert, D. *Phys. Rev. B* **1999**, *59*, 1758.

(18) Marini, A.; Hogan, C.; Gruning, M.; Varsano, D. *Comp. Phys. Comm.* **2009**, *180*, 1392–1403.

(19) Giannozzi, P.; Baroni, S.; Bonini, N.; Calandra, M.; Car, R.; Cavazzoni, C.; Ceresoli, D.; Chiarotti, G. L.; Cococcioni, M.; Dabo, I. *J. Phys.: Condens. Matter* **2009**, *21*, 395502 (19pp).

(20) Monkhorst, H. J.; Pack, J. D. *Phys. Rev. B* **1976**, *13*, 5188–5192.

(21) Shan, B.; Cho, K. *Phys. Rev. B* **2004**, *70*, 233405.

(22) Yang, L.; Deslippe, J.; Park, C.-H.; Cohen, M. L.; Louie, S. G. *Phys. Rev. Lett.* **2009**, *103*, 186802.

(23) Fox, M. *Optical properties of solids*; Oxford University Press, New York, 2001.

(24) Beal, A.; Hughes, H. *J. Phys. C: Solid State Phys.* **1979**, *12*, 881–890.